Monolithically Integrated Holmium Lasers on Silicon Chips

Nanxi Li[1,2,*], E. Salih Magden[1], Zhan Su[1,3], Neetesh Singh[1], Alfonso Ruocco[1], Ming Xin[1], Matthew Byrd[1,3], Patrick T. Callahan[1], Jonathan D. B. Bradley[1,4], Diedrik Vermeulen[1,3], and Michael R. Watts[1]

[1]*Research Laboratory of Electronics, Massachusetts Institute of Technology, 77 Massachusetts Avenue, Cambridge, MA 02139, USA*
[2]*John A. Paulson School of Engineering and Applied Science, Harvard University, 29 Oxford Street, Cambridge, MA 02138, USA*
[3]*Current address: Analog Photonics, One Marina Park Drive, Boston, MA 02210, USA*
[4]*Current address: Department of Engineering Physics, McMaster University, 1280 Main Street West, Hamilton, Ontario L8S 4L7, Canada*
**Corresponding author: nanxili@mit.edu*

Abstract: We demonstrate holmium-doped DFB lasers monolithically integrated on silicon. Single mode lasing at wavelength from 2.02 to 2.10 μm with 15 mW maximum output power are reported. This work extends silicon-photonic microsystems beyond 2 μm.

OCIS codes: (130.3120) Integrated optical devices; (140.0140) Lasers and laser optics; (230.5750) Resonators.

Wavelengths in the region of >2.0 μm have multiple atmospheric transmission windows, strong water absorption, and highly efficient mid-infrared (IR) frequency conversions. Hence, laser sources at these wavelengths enable a wide range of applications in the fields of medicine, LIDAR systems, remote sensing, trace-gas detection, and mid-IR wavelength generation [1, 2]. Thulium doped waveguide lasers operate most efficiently around 1.9 μm [3-5], while their efficiency at longer wavelengths is significantly reduced because of the diminishing emission cross-section of thulium doped gain media. In contrast, holmium doped lasers have an emission spectrum spanning from 1.95 to 2.15 μm, allowing for signal generation in this longer wavelength range [6-8] with a potential to be in-band-pumped using mature thulium laser technology [7].

In this paper, we demonstrate a holmium-doped distributed feedback (DFB) laser fabricated on a wafer-scale silicon photonics platform. We achieve single-mode lasing at wavelength longer than 2.02 μm with a side-mode suppression ratio of larger than 50 dB. The maximum on-chip lasing power is 15 mW with a slope efficiency of 2.3%. In addition, lasing wavelength control within the gain bandwidth of Al_2O_3:Ho^{3+} film is demonstrated by changing the gain film thickness. This is, to the best of our knowledge, the first holmium-doped integrated laser demonstrated on a complementary metal-oxide-semiconductor (CMOS)-compatible silicon photonics platform.

A wavelength-insensitive waveguide design [9] is used as gain waveguide of laser, which consists of five Si_3N_4 bars buried under SiO_2 with a layer of Al_2O_3:Ho^{3+} deposited on top, as shown in Fig. 1(a). The width and separation of the Si_3N_4 bars are optimized to provide high mode confinements within the Al_2O_3:Ho^{3+} film. The refractive indices of the materials at 2 μm are listed in Fig. 1(b). The TE field intensities of the fundamental mode at both the pump and signal wavelengths are shown in Fig. 1(c). A perspective view of the DFB laser is illustrated in Fig. 1(d). The lateral gap between grating and gain waveguide is designed to be 450 nm, and the grating width is chosen to be 260 nm to provide enough feedback at the designed laser wavelength. The total length of the cavity is 2 cm. The n_{eff} of the guided mode is calculated to be 1.552 at 2100 nm. Therefore, the corresponding grating period (Λ) can be calculated using $\lambda/2n_{eff}$. The transmission response of the DFB cavity is calculated by using transfer matrix method [10], as shown in Fig. 1(e). The lasers were fabricated in a state-of-the-art CMOS foundry. Al_2O_3:Ho^{3+} thin film is deposited at the top as a back-end-of-line process [11]. An SEM image of the Si_3N_4 layer is shown in Fig. 1(f).

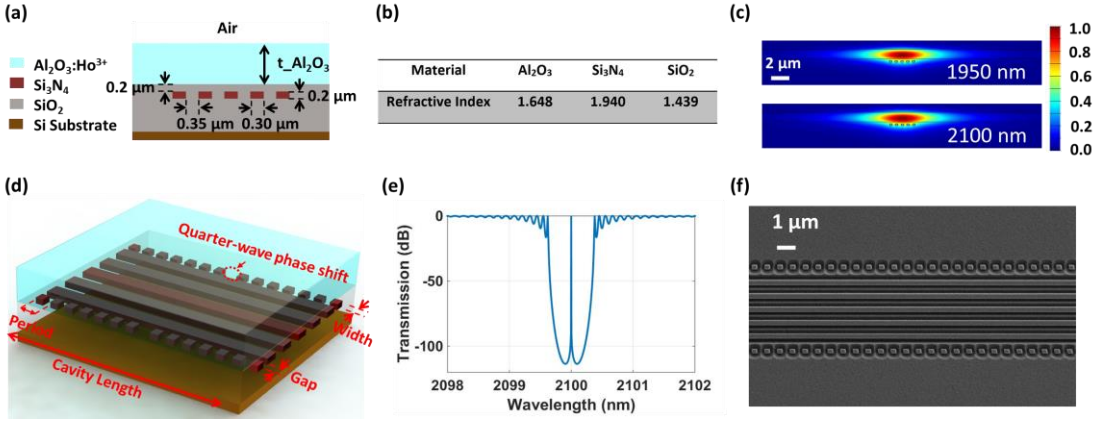

Figure 1. (a) Cross-sectional view of the laser waveguide. (b) Refractive indices of the waveguide materials. (c) Transverse-electric (TE) field intensities for the fundamental mode at both the pump and signal wavelengths. (d) A 3D illustration of the DFB laser (not to scale). (e) Transmission spectrum of the designed DFB cavity at 2100 nm. (f) An SEM image of the Si_3N_4 pattern (top view).

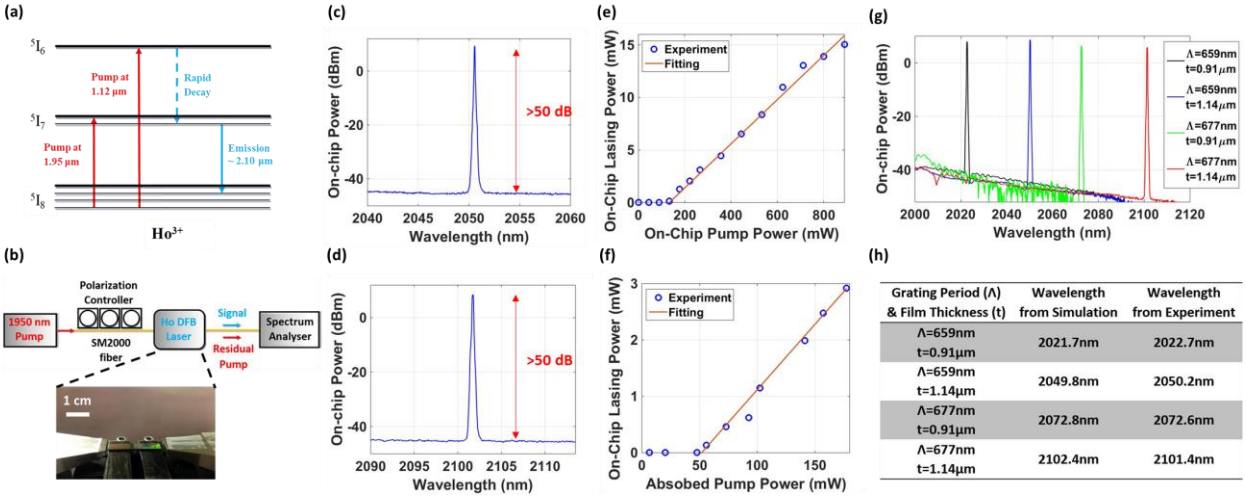

(h)

Grating Period (Λ) & Film Thickness (t)	Wavelength from Simulation	Wavelength from Experiment
Λ=659nm t=0.91μm	2021.7nm	2022.7nm
Λ=659nm t=1.14μm	2049.8nm	2050.2nm
Λ=677nm t=0.91μm	2072.8nm	2072.6nm
Λ=677nm t=1.14μm	2102.4nm	2101.4nm

Figure 2. (a) Ho^{3+} ion energy level diagram. (b) The characterization setup. (c)(d) The output spectra of the DFB lasers at 2051 nm and 2101 nm. (e)(f) DFB laser output power with respect to on-chip pump power and absorbed pump power (near lasing threshold). (g) Lasing wavelength control by changing the gain film thickness. (h) Comparison of lasing wavelength from simulation and experiment.

The Ho^{3+} ion energy diagram is shown in Fig. 2 (a). Pumping of the $^4I_7$ level can be addressed by 1.12 μm laser diodes [8] or ytterbium fiber lasers [12]. Alternatively, the $^5I_7$ level can be accessed by thulium lasers with a higher quantum efficiency. The characterization setup of the lasers is shown in Fig. 2(b). Two DFB lasers are designed with grating periods of 659 nm and 677 nm, corresponding to wavelengths around 2051 nm and 2101 nm, respectively. The measured lasing spectra of the DFB designs are shown in Fig. 2(c) and (d). The maximum on-chip output power was measured to be 15 mW, as shown in Fig. 2(e). The output power was measured from a single side of the laser with the fiber-to-chip coupling loss excluded. We obtained a slope efficiency of 2% and a lasing threshold of 130 mW. The lasing power near the threshold with respect to absorbed pump power is shown in Fig. 2(f), demonstrating a lasing threshold of 50mW and a slope efficiency of 2.3% with respect to the absorbed pump power. Furthermore, based on the same grating designs, by changing the gain film thickness from 1.14 μm to 0.91 μm through reducing the sputtering time in a new deposition run, we achieved lasing wavelength shifts from 2050.2 nm to 2022.7 nm and 2101.4 nm to 2072.6 nm, respectively, as shown in Fig. 2(g). Besides, the comparisons of lasing wavelengths between simulation and experiment are shown in Fig. 2(h), demonstrating an agreement within 1 nm. The difference may be caused by the thermal shift of the device [13], or the Al_2O_3 film thickness non-uniformity along the DFB cavity [14, 15].

In summary, we have demonstrated holmium doped DFB lasers monolithically integrated on a silicon chip. Single-mode lasers with wavelengths at 2051 nm and 2101 nm are obtained. By changing the gain film thickness, the lasing wavelength can be shifted. With 1950 nm pumping, a laser output power of 15 mW was measured with a slope efficiency of 2.3%.

This work was supported by Defense Advanced Research Projects Agency (DARPA) Direct On-Chip Digital Optical Synthesizer (DODOS) project (program manager: Dr. Gordon Keeler). N. Li acknowledges a fellowship from Agency of Science, Technology and Research (A*STAR), Singapore.

[1] S. L. K. Scholle, *et al.*,"2 μm Laser Sources and Their Possible Applications," in *Frontiers in Guided Wave Optics and Optoelectronics*, B. Pal, Ed., ed: InTech, 2010, 471-500.
[2] J. H. Taylor, *et al.*, "Atmospheric Transmission in the Infrared," *J. Opt. Soc. Am.* **47**, 223-226 (1957).
[3] K. Dalfsen, *et al.*"Thulium channel waveguide laser in a monoclinic double tungstate with 70% slope efficiency,"*Opt. Lett.* **37**, 887-889 (2012).
[4] K. Dalfsen, *et al.* "Thulium channel waveguide laser with 1.6W of output power and 80% slope efficiency," *Opt. Lett.* **39**, 4380-4383 (2014).
[5] N. Li, *et al.*, "High-power thulium lasers on a silicon photonics platform," *Opt. Lett.* **42**, 1181-1184 (2017).
[6] J. Wu, *et al.*, "Single frequency fiber laser at 2.05 μm based on Ho-doped germanate glass fiber," Proc. SPIE 7195, Fiber Lasers VI: Technology, Systems, and Applications, 71951K (Feb. 2009).
[7] A. Hemming, *et al.*,"High power operation of cladding pumped holmium-doped silica fibre lasers," *Opt. Express* **21**, 4560-4566 (2013).
[8] S. Jackson, *et al.*, "High-power and highly efficient diode-cladding-pumped Ho3+-doped silica fiber lasers," *Opt. Lett.* **32**, 3349-3351 (2007).
[9] Purnawirman, *et al.* "Ultra-narrow-linewidth Al2O3:Er3+ lasers with a wavelength-insensitive waveguide design on a wafer-scale silicon nitride platform," *Opt. Express* **25**, 13705-13713 (2017).
[10] T. E. Murphy, "Design, fabrication and measurement of integrated Bragg grating optical filters," Ph.D. Thesis, Massachusetts Institute of Technology, Cambridge, 2001.
[11] E. S. Magden, *et al.*,"Monolithically-integrated distributed feedback laser compatible with CMOS processing," *Opt. Express* **25**, 18058-18065 (2017).
[12] A. Shirakawa, *et al.*, "High-power Yb-doped photonic bandgap fiber amplifier at 1150-1200 nm," *Opt. Express* **17**, 447-454 (2009).
[13] N. Li, *et al.*, "Athermal synchronization of laser source with WDM filter in a silicon photonics platform," *Appl. Phys. Lett.* **110**, 211105 (2017).
[14] Purnawirman, *et al.* "Reliable Integrated Photonic Light Sources Using Curved Al2O3:Er3+ Distributed Feedback Lasers," *IEEE Photon. J.* **9**, 1-9 (2017).
[15] S. Swann, "Film thickness distribution in magnetron sputtering," *Vacuum* **38**, 791-794 (1988).